The Centrifugal Instability of a Slender Rotating Cone

Z. Hussain S. O. Stephen and S. J. Garrett

reprinted from

Journal of
Algorithms & Computational Technology

Volume 6 · Number 1

March 2012

Multi-Science Publishing Co. Ltd

The Centrifugal Instability of a Slender Rotating Cone

Z. Hussain[1,*] S. O. Stephen[2] and S. J. Garrett[1]
[1]Department of Mathematics, University of Leicester, UK.
[2]School of Mathematics, University of Birmingham, UK.

Received: 15/09/2010; Accepted: 18/03/2011

ABSTRACT

In this study, we provide a mathematical description of the onset of counter-rotating circular vortices observed for a family of slender rotating cones (of half-angles 15° or less) in quiescent fluid. In particular, we apply appropriate scalings in order to simplify the basic-flow profiles, which are subsequently perturbed, accounting for the effects of streamline curvature. A combined large Reynolds number and large vortex wavenumber analysis is used to obtain an estimate for the asymptotic right-hand branch of neutral stability for a slender rotating cone. Our results confirm our earlier predictions pertaining to the existence of the new Görtler mode and capture the effects of the governing centrifugal instability mechanism. Meanwhile, favourable comparisons are drawn with existing numerical neutral stability curve results.

1. INTRODUCTION

Recently, there has been considerable interest in the exact mechanisms governing the instability and transition to turbulence of flow in three-dimensional boundary layers. The rotating-disk has been used widely to model swept-wing flow due to similarities between their basic-flow profiles, but few studies exist on the boundary-layer flow over rotating cones. Comprehensive reviews covering geometries ranging from swept-wings to rotating disks and spheres are given by Reed & Saric [1], Saric et al. [2] and Reshotko [3]. Meanwhile, recent developments on spinning projectiles, aerofoils and

*Corresponding author. zh33@le.ac.uk.

aeroengines have furthered understanding of the onset of laminar-turbulent transition of boundary-layer flows over rotating cones.

Physically, laminar-turbulent transition within the boundary layer over a slender rotating nose cone can lead to significant increases in drag. For spinning projectile applications, such as missiles and torpedoes, the implications for control and accurate targeting are negative. Understanding the stability of such boundary-layer flows leads to design modifications and significant cost savings. As such, the rotating cone setup models the nose of a missile head travelling through the atmosphere, with ogive-nose cones (studied by Kohama [4] and Mueller et al. [5]) representing more realistic aerodynamic designs of modern missile heads.

The first experimental work on the rotating cone was conducted by Kreith, Ellis & Giesing [6], Tein & Campbell [7] and Kappesser, Greif & Cornet [8] for a rotating cone in still fluid, and by Salzberg & Kezios [9] for a rotating cone in axial flow, which is found to exhibit a stabilising effect on the flow to disturbances. While these experiments accurately measured Reynolds numbers for transition to turbulence, they were unable to sufficiently resolve the mechanisms at work within the laminar-turbulent flow region.

In the 1980s, experimental studies by Kobayashi et al. [10] and Kobayashi & Izumi [11] as well as by Kohama [4] and Mueller et al. [5] (for ogive-nose cones) observed the existence of spiral vortices, which are generated in the region of steep shear velocity gradients near the cone wall. Using high-speed strobe light flow visualisation techniques, these studies showed in detail the spiral vortices being shed from the cone boundary layer under the action of distorting forces from the mean velocity field.

It was noticed that a key influence on the nature of these vortices is the cone half-angle. For example, the experimental study by Kobayashi & Izumi [11] for cones with slender half-angles, ψ, as low as 15°, clearly show the existence of pairs of counter-rotating Görtler vortices, which arise from a dynamic instability induced by the centrifugal force of the flow field (as shown in figure 1). However, for $\psi > 30°$, their results clearly show the spiral vortices transform to more familiar co-rotating crossflow vortices.

Indeed, measurements of the spiral angle (the angle between the normal to the vortices and the cone meridian) by Garrett et al. [12] are shown to approach those observed for a rotating disk as the half-angle tends to 90°. It is well-known from the studies of Gregory et al. [13] and Hall [14] that the stationary spiral vortices observed on the rotating disk are in fact co-rotating vortices attributed to an underlying crossflow instability, based on an unstable inflexion

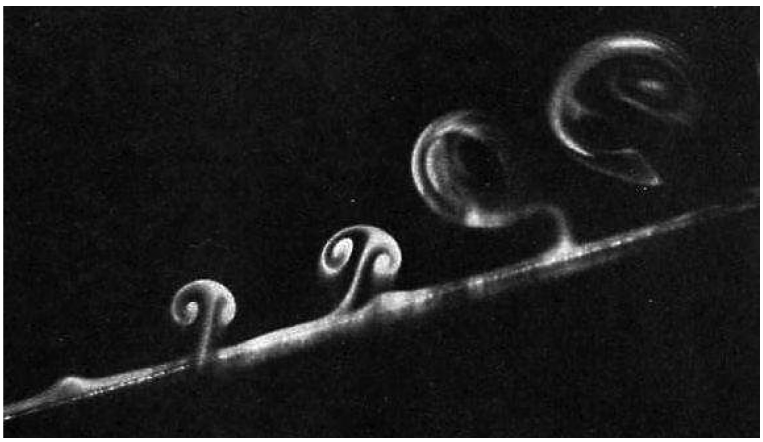

Figure 1. Cross-sectional flow visualisation showing pairs of counter-rotating Görtler vortices at $\psi = 15°$ (Kobayashi & Izumi 11]).

point in the crossflow component of the flow field. Recently, Garrett et al. [12] suggested that the observed centrifugal instability for slender cones with $\psi < 40°$ stems from an inherently different process to that governing the crossflow instability for cones with $\psi > 40°$. Therefore, there is a distinct variation in the underlying physical mechanism governing the instability for slender cones, which we shall identify here and model.

The Görtler instability is a type of centrifugal mechanism, which occurs in the presence of wall curvature. When the boundary layer thickness is small compared with the radius of curvature, the flow instability is visualised through the formation of Görtler vortices, which break down to form successive pairs of counter-rotating vortices. Early work on the Görtler instability mechanism concerned the linear stability of two-dimensional flows over concave walls, for example by Görtler [15] and Smith [16]. The parallel-flow approximation was used, and higher-order curvature effects were neglected. Later, Hall [17] considered non-parallel effects in the basic flow and found that the disturbances are concentrated in internal viscous or critical layers well away from the wall and the free stream. Further numerical investigations by Hall [18, 19] for nonlinear non-parallel vortices in growing boundary layers led to a characterisation of the three-dimensional effects of the centrifugal Görtler instability mechanism. Importantly, it was observed that the relative size of the crossflow and chordwise flow determines the vortex structure. Hence, by scaling the coordinates spanwise and normal to the vortex structures on the

boundary layer thickness, it is possible to develop a linear analysis of neutral modes characterised by a large vortex wavenumber.

A comprehensive review of these studies may be found in Hall [20], where the receptivity problem for Görtler vortices impinging on the leading edge of the wall was also considered. In a later study, Bassom & Hall [21] analysed the effect of altering the amount of crossflow present in a boundary-layer as a mechanism for representing the degree of three-dimensionality within the flow in both small-and large-wavenumber limits. It was found that sufficiently strong levels of crossflow eventually eradicate the presence of the Görtler instability mechanism within the boundary layer. This is of particular interest in the boundary-layer flow over a rotating cone, as we see from the experiments of Kobayashi & Izumi [11] that the centrifugal Görtler instability for small ψ is eventually visualised as a crossflow dominated instability for larger values of ψ. We identify the counter-rotating vortices for small ψ observed by Kobayashi & Izumi [11] as pairs of Görtler vortices and suggest that, as in the study of Bassom & Hall [21], increasing the level of crossflow (by increasing ψ) eventually leads to the eradication of the counter-rotating Görtler vortex pairs.

This paper forms the first part of a series of studies investigating the centrifugal Görtler instability mechanism for slender rotating cones; future studies will concentrate on the helical spiral waves for larger half-angles ($15° < \psi < 45°$), which have been observed by Kobayashi & Izumi [11] as well as slender rotating cones in axial flow (see Kobayashi et al. [10] and Kobayashi [22]). In the present study, we setup the formulation in section 2 for a slender half-angle rotating cone in still fluid and derive the steady flow equations in section 2.1. We proceed to apply appropriate scalings to capture the effects of streamline curvature in section 2.2 leading to the disturbance equations; these form the basis of a large Reynolds number and large vortex wavenumber stability analysis presented in section 3, with a physical interpretation of the results in section 4. Finally in section 5, we develop comparisons between our results and existing numerical calculations obtained by Kobayashi & Izumi [11], before expanding on additional work in progress.

2. FORMULATION

We consider a rotating cone setup where the half-angle ψ is sufficiently small ($\psi \leq 15°$) for the dominant mechanism governing the primary instability to arise from centrifugal forces in the mean flow, due to the curvature of the cone surface. In particular, flow visualisation of the instability in the literature is

distinguished by the existence of two physical cases: the existence circular waves aligned parallel to the azimuthal axis and helical spiral waves, which appear oblique to the azimuthal axis (see Kobayashi & Izumi [11]). Here, we proceed to outline the coordinate setup to successfully model circular vortex waves with zero growth.

2.1 The Steady Flow

Consider a rigid cone of infinite extent with half-angle ψ, rotating about its axis of symmetry with constant angular velocity Ω^* in a fluid of kinematic viscosity ν^*. We choose an orthogonal curvilinear coordinate system which rotates with the cone (x, θ, z), representing streamwise, azimuthal and surface-normal variation, respectively. The local cross-sectional radius of the cone is given by $r^* = x^* \sin \psi$ (where * denotes dimensional quantities).

Length quantities are scaled on a characteristic length along the cone surface, l^*, and the surface-normal coordinate is further scaled on the boundary-layer thickness $(\nu^*/\Omega^* \sin \psi)^{1/2}$:

$$x^* = l^* x,\ z^* = l^* z,\ z = R^{-1/2}\eta. \tag{1}$$

where η is the non-dimensional wall-normal coordinate within the boundary layer and R is the Reynolds number, defined by

$$R = \frac{\Omega^* l^{*2} \sin\psi}{\nu^*}. \tag{2}$$

The steady velocities are non-dimensionalised using the local surface velocity, $x^*\Omega^* \sin \psi$, so the axisymmetric mean flow is

$$\mathbf{u} = \mathbf{u}_b = \Omega^* l^* \sin\psi\,(xU(\eta)), xV(\eta), R^{-1/2}W(\eta)), \tag{3}$$

where U, V and W are the non-dimensional velocities in the x^*, θ and z^* directions respectively. We scale the steady pressure as

$$p^* = p_b^* = \rho^* \Omega^{*2} l^{*2} \sin^2 \psi(P_0(x) + R^{-1/2} xP(\eta)), \tag{4}$$

The relevant continuity and Navier-Stokes equations for the cone geometry are non-dimensionalised using equations (1–4). Expanding the governing equations in terms of R and ignoring terms $O(R^{-1/2})$, leads to the familiar von Kármán [23]

equations for boundary-layer flow over a rotating disk, and an additional equation for the pressure:

$$W' + 2U = 0, \tag{5}$$

$$WU' + U^2 - (V+1)^2 = U'', \tag{6}$$

$$WV' + 2U(V+1) = V'', \tag{7}$$

$$(V+1)^2 \cot\psi = \frac{dP}{d\eta}, \tag{8}$$

with boundary conditions

$$\begin{aligned} U = 0, V = 0, W = 0, \quad \text{on } \eta = 0, \\ U \to 0, V \to -1, \quad \text{as } \eta \to \infty. \end{aligned} \tag{9}$$

Note that a prime denotes differentiation with respect to η. Consequently, we note that this choice of non-dimensionalization results in ψ being scaled out of the steady flow equations (5–8) for fluid velocity. The system of equations (5–8) subject to boundary conditions (9) is solved using a fourth-order Runge-Kutta integration method, in conjunction with a two-dimensional Newton-Raphson searching routine. We iterate on the boundary conditions at infinity to produce the well-known velocity profiles.

2.2 Linear Disturbance Equations

To model the slender cone problem, we shall consider the special case where circular waves have been observed experimentally for a rotating cone of half-angle $\psi = 15°$ by Kobayashi & Izumi [11]. In still fluid, these waves are aligned with the azimuthal axis (θ), and as such are periodic in the streamwise direction (x). Hence, a linear stability analysis incorporating curvature effects may be developed.

We proceed to linearize the governing equations about the von Kármán steady mean flow profile (3) and the basic fluid pressure (4) by introducing small perturbation quantities. To obtain the form of these quantities and capture the effects of streamline curvature, we first scale the streamwise and normal coordinates on boundary layer thickness, in the form

$$\eta = R^{1/2} z, \quad \bar{x} = R^{1/2} x. \tag{10}$$

These scales are physically consistent with research in the literature for problems where the Görtler instability has been modelled, as summarized by Hall [20]. Streamwise and normal coordinates are scaled on the boundary layer thickness, as they proceed in spanwise and perpendicular directions to the circular Görtler vortices. Next, we use the fact that the vortices are periodic in the streamwise direction to introduce perturbation quantities, which are characterised by a vortex wavenumber a and azimuthal wavenumber b. Our basic flow quantities remain unchanged, whereas we scale the perturbation velocities on boundary layer thickness, so that $\mathbf{u}$ and p^* may be expressed according to:

$$\mathbf{u} = \mathbf{u}_b + \tilde{\mathbf{u}}, \quad p^* = p_b{}^* + \tilde{p}^*, \tag{11}$$

where

$$\mathbf{u} = (\Omega^* l^* \sin\psi) R^{-1/2} \{u(\eta), v(\eta), w(\eta)\} \exp(\mathrm{i}a\bar{x} + \mathrm{i}b\theta), \tag{12}$$

and the pressure perturbation term scales as

$$p^* = (\rho^* \Omega^{*2} l^{*2} \sin^2 \psi) R^{-1} p(\eta) \exp(ia\bar{x} + ib\theta). \tag{13}$$

We non-dimensionalise the governing time-dependent Navier-Stokes equations and proceed to ignore nonlinear terms. As a result, this choice of scaling leads to a set of linearized perturbation equations. We note that scaling the velocity and pressure quantities on boundary layer thickness and its square, respectively, ensures the resulting leading-order perturbation equations are independent of the Reynolds number, R. Furthermore, this is the only such choice of scaling, which leads to consistent disturbance equations. Hence, we apply a large Reynolds number assumption in order to recover the leading-order equations. Our subsequent task is to investigate the short-wavelength asymptotic structure of the centrifugal instability. We identify the spiral vortex wavenumber as $a = \varepsilon^{-1}$, where ε is a small parameter which forms the basis of our asymptotic analysis, and $b = O(1)$. Therefore, the study develops into a combined large Reynolds number and small wavelength asymptotic analysis, where Görtler modes are investigated for both large R and small ε. After applying this substitution, we differentiate the x-component equation with respect to η and use the z-component equation to arrive at the following form for the reduced system of linearized disturbance equations

$$iu+\epsilon\left(\frac{u\sin\psi+w\cos\psi}{\bar{h}}\right)+\mathrm{i}\frac{b\epsilon v}{\bar{h}}+\epsilon\frac{\partial w}{\partial\eta}=0, \tag{14}$$

$$\left(\epsilon^2\frac{\partial^2}{\partial\eta^2}-1\right)^2 w=2\epsilon^2\left(\frac{\bar{x}V\sin\psi}{\bar{h}}+1\right)v\cot\psi$$

$$-\mathrm{i}\epsilon^3\frac{\partial^2\tilde{u}}{\partial t\partial\eta}+\frac{\partial}{\partial\eta}\left(\epsilon^2\bar{x}U\tilde{u}+\frac{b\epsilon^3\bar{x}V}{\bar{h}}\tilde{u}-\mathrm{i}\epsilon^3W\frac{\partial\tilde{u}}{\partial\eta}\right.$$

$$\left.-\mathrm{i}\epsilon^3Uu-\mathrm{i}\epsilon^3w\bar{x}U'+2\mathrm{i}\epsilon^3\left[\frac{\bar{x}V\sin\psi}{\bar{h}}+1\right]v\right)$$

$$-\left(\epsilon^2\frac{\partial w}{\partial t}+\mathrm{i}\epsilon\bar{x}Uw+i\frac{b\epsilon^2\bar{x}V}{\bar{h}}w+\epsilon^2W\frac{\partial w}{\partial\eta}\right)-2\epsilon^2\left[\frac{\bar{x}V\sin\psi}{\bar{h}}+1\right]v\cot\psi$$

$$+\frac{b^2\epsilon^2}{\bar{h}^2}w-\mathrm{i}\frac{\epsilon\sin\psi}{\bar{h}}w-\frac{\epsilon^2\cos\psi}{\bar{h}}\frac{\partial w}{\partial\eta}+\frac{\epsilon^2(u\sin\psi+w\cos\psi)}{\bar{h}^2}\cos\psi+2\mathrm{i}\frac{b\epsilon^2\cos\psi}{\bar{h}^3}v$$

$$+\epsilon^2\frac{\partial}{\partial\eta}\left(\frac{u\sin\psi+\mathrm{i}bv+w\cos\psi}{h}\right)-\epsilon^4\frac{\partial^3}{\partial\eta^3}\left(\frac{u\sin\psi+\mathrm{i}bv+w\cos\psi}{h}\right)$$

$$-\mathrm{i}\left(\frac{\epsilon^3b^2}{\bar{h}^2}\frac{\partial\tilde{u}}{\partial\eta}-\mathrm{i}\frac{\epsilon^2\sin\psi}{\bar{h}}\frac{\partial\tilde{u}}{\partial\eta}-\frac{\epsilon^3\cos\psi}{\bar{h}}\frac{\partial^2\tilde{u}}{\partial\eta^2}+\frac{\epsilon^3}{\bar{h}^2}\left[\frac{\partial\tilde{u}}{\partial n}\sin\psi+\frac{\partial\tilde{w}}{\partial\eta}\cos\psi\right]\sin\psi\right), \tag{15}$$

$$\left(\epsilon^2\frac{\partial^2}{\partial\eta^2}-1\right)v=\epsilon^2\bar{x}wV'+\epsilon^2\frac{\partial v}{\partial t}+\mathrm{i}\epsilon\bar{x}Uv+\mathrm{i}\frac{b\epsilon^2\bar{x}V}{\bar{h}}v+\epsilon^2W\frac{\partial v}{\partial\eta}+\epsilon^2Vu$$

$$+\frac{\epsilon^2}{\sin\psi}\left(\frac{\bar{x}V\sin\psi}{\bar{h}}+2\right)(u\sin\psi+w\cos\psi)+\epsilon^2\left(\frac{\bar{x}U\sin\psi+W\cos\psi}{\bar{h}}\right)v$$

$$+\mathrm{i}\frac{b\epsilon^2}{\bar{h}}\tilde{p}+\frac{(b^2+1)\epsilon^2}{\bar{h}^2}\tilde{v}-\mathrm{i}\frac{\epsilon\sin\psi}{\bar{h}}\tilde{v}-\frac{\epsilon^2\cos\psi}{\bar{h}}\frac{\partial\tilde{v}}{\partial\eta}$$

$$-2\mathrm{i}\frac{b\epsilon^2\sin\psi}{\bar{h}^3}\tilde{u}-2\mathrm{i}\frac{b\epsilon^2\cos\psi}{\bar{h}^3}\tilde{w}, \tag{16}$$

subject to the boundary conditions

$$u=v=w=0,\quad \text{on}\quad \eta=0,\infty, \tag{17}$$

where $\bar{h}=R^{1/2}(x\sin\psi+z\cos\psi)$.

3. NEUTRAL STABILITY MODES

In order to conduct a linear stability analysis, the approach we use is to asymptotically expand the disturbance quantities and apply the method of matched asymptotic expansions. Importantly, we are conducting a combined asymptotic stability analysis for large Reynolds number R and large vortex wavenumber ε^{-1}. As a result, we require a single parameter to suitably capture the physical effect of both asymptotically large quantities, which we will introduce in section 3.1 as the Taylor number, T. To analyse the neutrally stable perturbations with zero growth appearing in the governing equations (14–16), we observe that the steady flow problem setup is similar to the investigation of Hall [17] for the Taylor problem of flow between concentric rotating cylinders. We follow the analysis of Hall [17] for the Taylor problem by expanding the perturbation quantities and the Taylor number, which is defined as $T = 2 \cot \psi$, and given by the balance of centrifugal forces from the cone rotation and viscous forces. Furthermore, as we shall develop an asymptotic analysis for large Taylor number, we note the quantity $2 \cot \psi$ becomes large for a slender cone, where ψ is small. Now, in a similar way to Hall [17] for the Taylor problem, we follow Meksyn [24] and seek a WKB solution corresponding to the case $\varepsilon \to 0$ and obtain a balance of the dominant terms provided we scale $T \sim \varepsilon^{-4}$ and $W/V \sim O(\varepsilon^{-2})$, resulting in

$$\begin{aligned}
\tilde{u} &= E(u_0(\eta) + \epsilon u_1(\eta) + \epsilon^2 u_2(\eta) + \ldots), \\
\tilde{v} &= \epsilon^2 E(v_0(\eta) + \epsilon v_1(\eta) + \epsilon^2 v_2(\eta) + \ldots), \\
\tilde{w} &= E(w_0(\eta) + \epsilon w_1(\eta) + \epsilon^2 w_2(\eta) + \ldots), \\
T &= \epsilon^{-4}(T_0 + T_1\epsilon + T_2\epsilon^2 + \ldots),
\end{aligned} \tag{18}$$

where

$$E = \exp \frac{\mathrm{i}}{\epsilon} \int^{\eta} K(\tau) \mathrm{d}\,\tau. \tag{19}$$

3.1 Leading Order Solution

After substituting the above expressions into equations (15), (16) and equating terms of $O(1)$ and $O(\varepsilon^2)$ respectively, we arrive at the following eigenrelation at leading order

$$(K^2 + 1)^3 = \frac{T_0 \bar{h}}{\sin\psi} \left(\frac{\bar{x} V \sin\psi}{\bar{h}} + 1 \right) \frac{\bar{x} \sin\psi}{\bar{h}} V'. \tag{20}$$

Following the Taylor analysis developed by Hall [17], the vortex activity is located at the wall, and as such the rotating cone analysis is consistent, so that $V(0) = 0$. Consideration of the eigenfunctions corresponding to the six roots of equation (20) (see Meksyn [24]) show that only real values of K result in acceptable solutions to the stability equations. Further details are omitted here, but in brief, we argue as in Hall [17] that real values of K occur in regions where the right-hand side of equation (20) is positive and has its greatest magnitude. After re-scaling the eigenvalue in the form $\overline{T} = T\overline{x}$, we obtain the leading order eigenvalue estimate $\overline{T}_0 = -V'^{-1}_{\min}$, where the minimum $V'_{\min} = V'(0) = -0.6159$ occurs at the wall where $\eta = 0$. Therefore, for a slender cone with $\psi = 15°$, where purely circular waves are observed in still fluid, the leading order eigenvalue estimate is $\overline{T}_0 = 1.6236$.

3.2 First Order Solution

Our next task is to investigate the asymptotic structure of the effective scaled Taylor number, $\overline{T} = T\overline{x}$, for the special case when $\overline{T}_0 = -V'(0)^{-1}$. We apply the differential operator $(\epsilon^2\partial^2/\partial\eta^2 - 1)$ to (15) and use equation (16) to simplify by eliminating relevant terms in $\tilde{v}$, leading to

$$\left(\epsilon^2\frac{\partial^2}{\partial\eta^2}-1\right)^3 w = \epsilon^4 T\left(\frac{\overline{x}V\sin\psi}{\overline{h}}+1\right)\overline{x}V'w + O(\epsilon), \tag{21}$$

subject to the boundary conditions

$$w = \frac{\partial^2 w}{\partial\eta^2} = \frac{\partial}{\partial\eta}\left(\epsilon^2\frac{\partial^2}{\partial\eta^2}-1\right)w = 0, \quad \eta = 0,\infty. \tag{22}$$

Here, a number of additional terms appear in equation (21), which for brevity are omitted, as they only play a role in the asymptotic expansions at higher order. However, for clarity the reader is referred to Hussain's PhD thesis [25]. We now follow the scalings used by Hall [17] for the Taylor problem and expand the Taylor number using a modified expansion to equation (18) given by

$$T = \epsilon^{-4}\left(T_0 + T_1\epsilon^{2/3} + \ldots\right). \tag{23}$$

While further details in the approach are similar to the analysis of Hall [17] for the Taylor problem, full details can be found in Hussain's PhD thesis [25]. Here, we emphasize distinctions between the analyses, which arise due to the differences in the steady flow profiles (3) and the definition for the Taylor number. In brief, we employ the method of matched asymptotic expansions to show that there exists a layer of thickness $\varepsilon^{2/3}$ where the solution which satisfies the boundary conditions (17) as $\eta \to \infty$ is governed by the Airy function.

However, in order to satisfy the boundary conditions at $\eta = 0$, an inner boundary layer exists of thicknessε. As a result, upon matching the inner layer solution with the outer boundary layer solution, we obtain the following eigenrelation

$$\mathrm{Ai}\left(-\frac{T_1\bar{x}3^{-1/3}}{|V'(0)|}\right)=0. \tag{24}$$

This results in an infinite sequence of eigenvalues $\{T_{1n}\}$, which correspond to the zeros of the Airy function on the negative real axis. Subsequently, the most dangerous mode of instability has a re-scaled effective Taylor number expansion given by

$$\begin{aligned}\bar{T} = T\bar{x} &= \epsilon^{-4}\left(\frac{1}{|V'(0)|}+2.3381|V'(0)|3^{1/3}\epsilon^{2/3}+\ldots\right),\\ &= \epsilon^{-4}\left(1.6236+2.0769\epsilon^{2/3}+\ldots\right).\end{aligned} \tag{25}$$

4. PHYSICAL INTERPRETATION

Qualitatively, this asymptotic expansion of the effective Taylor number (25) corresponds to an asymptotic estimate of the right-hand branch of the neutral stability curve. Furthermore, it represents cones of half-angle $\psi = 15°$, which admit circular waves aligned with the azimuthal axis, as observed in the experimental studies of Kobayashi & Izumi [11]. Hence, the result applies within a specific parameter regime to a small family of slender cones.

Physically, we observe that an increase in the vortex wavenumber of the circular waves is achieved by an increase in the Taylor number, which governs the flow, so we move further up the right-hand branch of the neutral curve. Our assumptions in the analysis require that the boundary layer instability develops

from close to the cone nose and grows in the streamwise direction. As the vortex streaks remain circular in nature, we propose that there is no growth along the azimuthal direction. Hence, for cones of half-angle ψ = 15°, the vortices are visualised as circular rings and, in terms of the centrifugal instability, the resulting flow structure is one of the most stable configurations. While the rotational shear effect of the spinning cone sheds vorticity in the azimuthal direction, the cone half-angle is sufficiently small such that the streamwise forcing of the mean flow causes vorticity to be shed along the cone. The result is the appearance of counter-rotating vortices, which form each individual streak on the cone surface as the instability develops. Indeed, the cone half-angle $\psi = 15°$ is a special case as it exhibits a flow arrangement where these counter-rotating Görtler vortex streaks remain aligned with each other as circular waves; these rings, termed 'Taylor' vortices by Kobayashi et al. [10], are also observed for a 15° cone in a range of axial flows.

We now present a comparison between our effective Taylor number estimate and existing results in the literature, which have been calculated by Kobayashi & Izumi [11], and are presented in terms of the rotational Reynolds number against the vortex wavenumber, referred to as σ. Now, for slender cones we know that the boundary layer instability is visualised in terms of counter-rotating spiral vortices (see Kobayashi & Izumi [11]), which are often termed Görtler vortices. Furthermore, Hall [17] shows that the Görtler number, G, which describes the governing centrifugal instability may be written in the form $G = 2R^{1/2}\delta$, with curvature term δ. Now, Hall [17] shows that $G = O(\varepsilon^{-4})$, whereas the scaled effective Taylor number estimate (25) gives $\bar{T} = O(\epsilon^{-4})$. Hence, we connect the rotational Reynolds number, Re, to the conventional Reynolds number, R, using equation (8) of Kobayashi & Izumi [11] to re-write the curvature term, which leads to the relation $Re = R^{1/2}\sqrt{(1.616)}$.

As a result, we may write the rotational Reynolds number in terms of the effective Taylor number $Re = \bar{T}\sqrt{(1.616)}$. This allows us to make a direct quantitative comparison between our asymptotic estimate for the scaled effective Taylor number and the numerical Reynolds number calculated by Kobayashi & Izumi [11], which is shown in Figure 2. Here, both quantities are calculated against the spiral vortex wavenumbers, referred to as ε^{-1} and σ, respectively. Kobayashi's data is displayed for low Reynolds number Re and low σ, whereas our results are valid for large Taylor number and large vortex wavenumber. Noting that our model employs the assumption of large Reynolds number, we see our comparisons with Kobayashi & Izumi [11] (for which data exists up to $Re \sim 500$) improve as the Reynolds number increases.

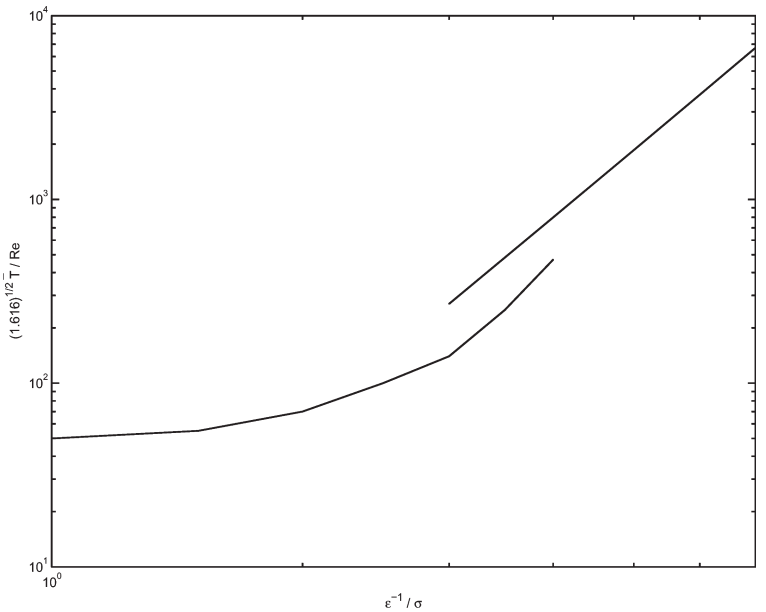

Figure 2. Comparison between scaled effective asymptotic Taylor number $\overline{T}$ (right) and Reynolds number *Re* of Kobayashi & Izumi [11] (left) against vortex wavenumbers ε^{-1} and σ for $\psi = 15°$.

We therefore conclude the current asymptotic setup closely models the right-hand branch of the neutral curve for Reynolds numbers of $O(10^4)$ and above.

5. CONCLUSION

We have non-dimensionalised the governing Navier-Stokes equations and introduced appropriate scalings to extract the effects of streamline curvature for a slender rotating cone. Subsequently, a combined asymptotic linear stability analysis for large Reynolds number and large vortex wavenumber has led to an expansion for the governing physical parameter, the Taylor number $T = 2 \cot \psi$, which corresponds to the right-hand branch of the neutral stability curve. The chosen scalings of the streamwise and normal coordinates, velocity and pressure perturbations all depend on the Reynolds number R, with the aim being to render the governing perturbation equations at leading order (14)–(16) independent of R. Hence, in the following asymptotic analysis outlined in section 3, the Taylor number T emerges as the main physical parameter in the

problem, governed by surface curvature. This is consistent with Hall [17], where the Taylor problem of flow between concentric cylinders is considered. Importantly, alternative scalings would not successfully identify T as the governing param-eter, as the perturbation equations would remain dependent on R. Initially a factor in the right-hand side of the first term in equation (15), T is asymptotically expanded to appear in the eigenrelation (20) at leading order and subsequently in the first-order perturbation equation (21), with an Airy function solution.

Once T has been identified as the governing physical parameter in the perturbation equations at leading order for large Reynolds number, it is asymptotically expanded in terms of large vortex wavenumber ε^{-1}, for small ε. As a result, the asymptotic expansion for T depends directly on ε, with the solution (25) being compared with the rotational Reynolds number Re of Kobayashi & Izumi [11] in section 4. Therefore, the initial choice of coordinate, velocity and pressure scales in terms of large Reynolds number R play a major role in casting the perturbation equations in a suitable form to enable a subsequent asymptotic analysis for small ε.

Importantly, the present study is confined to a family of slender cones rotating within still fluid. Work is currently underway to extend the range of applicability to less slender cones ($15° < \psi < 45°$),where the centrifugal instability is still believed to play a dominant role in still fluid (see Kobayashi & Izumi [11]). In addition, the introduction of a fixed strength axial flow models spinning projectiles with greater physical relevance; a stability analysis in this setup would involve using the more complex basic flows discussed in Garrett et al. [26]. Furthermore, both numerical and experimental studies by Kobayashi [22] and Kobayashi et al. [10] exist in the axial flow case, which facilitates comparisons with the asymptotics in progress; we hope to report on both studies in due course.

The authors are grateful to Prof. Choi-Hong Lai for the opportunity to present this paper at Greenwich, as well as the Department of Mathematics, University of Leicester, and the EPSRC for their financial support. The author is also grateful to the referee for providing useful comments on the first draft of this paper.

REFERENCES

1. Reed, H. L. & Saric, W. S., Stability of three-dimensional boundary layers, *Ann. Rev. Fluid Mech.*, 21, 235–284 (1989).
2. Saric, W. S., Reed, H. L. & White, E. B., Stability and transition of three-dimensional boundary layers, *Ann. Rev. Fluid Mech.*, 35, 413–440 (2003).

3. Reshotko, E., Boundary-layer instability, transition and control, *AIAA J.*, 94, 0001 (1994).
4. Kohama, Y., Flow structures formed by axisymmetric spinning bodies, *AIAA J.*, 23, 1445 (1985).
5. Mueller, T. J., Nelson, R. C., Kegelman, J. T. & Morkovin, M. V., Smoke visualisation of boundary-layer transition on a spinning axisymmetric body, *AIAA J.*, 19, 1607 (1981).
6. Kreith, F., Ellis, D. & Giesing, J., An experimental investigation of the flow engendered by a rotating cone, *Appl. Sci. Res.*, A11, 430–440 (1962).
7. Tein, C. L. & Campbell, D. T, Heat and mass transfer from rotating cones, *J. Fluid Mech.*, 17, 105–112 (1963).
8. Kappesser, R., Greif, R. & Cornet, I., Mass transfer on rotating cones, *Appl. Sci. Res.*, 28, 442–452 (1973).
9. Salzberg, F. & Kezios, S. P., Mass transfer from a rotating cone in axisymmetric flow, *J. Heat Transfer*, 87, 469–476 (1965).
10. Kobayashi, R., Kohama, Y. & Kurosawa, M., Boundary-layer transition on a rotating cone in axial flow, *J. Fluid Mech.*, 127, 341–352 (1983).
11. Kobayashi, R. & Izumi, H., Boundary-layer transition on a rotating cone in still fluid, *J. Fluid Mech.*, 127, 353–364 (1983).
12. Garrett, S. J., Hussain, Z. & Stephen, S. O., The crossflow instability of the boundary layer on a rotating cone. *J. Fluid Mech.*, 622, 209–232 (2009).
13. Gregory, N., Stuart, J. T. & Walker, W. S., On the stability of three-dimensional boundary layers with application to the flow due to a rotating disk, *Phil. Trans. R. Soc. Lond. A*, 248, 155–199 (1955).
14. Hall, P., An asymptotic investigation of the stationary modes of instability of the boundary layer on a rotating disk, *Proc. R. Soc. Lond. A*, 406, 93–106 (1986).
15. GÖRTLER, H., Uber eine dreidimensionale instabilität laminare Grenzschubten an Konkaven Wänden., *NACA TM*, 1357 (1940).
16. Smith, A. M. O., On the growth of Taylor–Görtler vortices along highly concave walls, *Q. Appl. Maths*, 13, 233–262 (1955).
17. Hall, P., Taylor-Görtler vortices in fully developed or boundary-layer flows: linear theory, *J. Fluid Mech.*, 124, 475–494 (1982).
18. Hall, P., The Görtler vortex instability mechanism in three-dimensional boundary layers, 1985, *Proc. R. Soc. Lond. A*, 299, 135–152 (1985).
19. Hall, P., The nonlinear development of Görtler vortices in growing boundary layers, 1988, *J. Fluid Mech.*, 193, 247–266 (1988).
20. Hall, P., Görtler vortices in growing boundary layers: the leading edge receptivity problem, linear growth and the nonlinear breakdown stage, *Mathematika*, 37,

151–189 (1990).
21. Bassom, A. P. & Hall, P., Vortex instabilities in three-dimensional boundary layers: the relationship between Görtler and crossflow vortices, *J. Fluid Mech.*, 232, 647–680 (1991).
22. Kobayashi, R., Linear stability theory of boundary layer along a cone rotating in axial flow, *Bull. JSME*, 24, 934–940 (1981).
23. KÁRMÁN, T. von, Uber laminare und turbulente Reiburg, *Z. Agnew. Math. Mech.*, 1, 233–252 (1921).
24. Meksyn, D., Stability of viscous flow between rotating cylinders. I, *Proc. R. Soc. Lond. A*, 187, 115–128 (1946).
25. Hussain, Z., *Stability and Transition of Three-dimensional Rotating Boundary Layers*, PhD Thesis, University of Birmingham (2010).
26. Garrett, S.J., Hussain, Z. & Stephen, S.O., Boundary-layer transition on broad cones rotating in an imposed axial flow, *AIAA J.*, 48, No. 6 (2010).